A micro-sphere-based remodelling formulation for soft tissue involving residual stresses

Andreas Menzel[1,2] **and Tobias Waffenschmidt**[3]

[1]*Institute of Mechanics, Department of Mechanical Engineering, TU Dortmund*
Leonhard-Euler-Str. 5, 44227 Dortmund, Germany
e-mail: andreas.menzel@udo.edu

[2]*Division of Solid Mechanics, Lund University*
P.O. Box 118, SE-22100 Lund, Sweden
e-mail: andreas.menzel@solid.lth.se

[3]*Institute of Mechanics, Department of Mechanical Engineering, TU Dortmund*
Leonhard-Euler-Str. 5, 44227 Dortmund, Germany
e-mail: tobias.waffenschmidt@udo.edu

Abstract

A three-dimensional micro-sphere-based constitutive model for anisotropic soft biological tissue is presented, which includes fibre-reorientation-related remodelling phenomena as well as residual stress effects. Within the underlying constitutive framework, the isotropic part of the strain energy is described by a conventional neo-Hooke-type model. The anisotropic contribution is reflected by the one-dimensional micro-mechanically based worm-like chain model, which by means of a micro-sphere approach can be extended to the three-dimensional case. As one key aspect of this contribution, time-dependent remodelling effects are incorporated by introducing evolution equations for the integration directions of the micro-sphere scheme, which thereby characterize the material's anisotropic properties. A computational remodelling approach for the orthotropic case with two fiber families will be developed. As another key aspect, the effect of residual stresses is additionally included in the model by means of a multiplicative decomposition of the deformation gradient tensor. In order to underline the applicability of the proposed constitutive model with regard to iterative finite element schemes and to validate the results, several numerical studies of representative boundary value problems are presented.

Keywords: anisotropy, biomechanics, large deformations, solid mechanics, non-linear elasticity

1. Introduction

An essential property of fibrous biological tissues in vivo is the ability to adapt according to respective loading conditions—for example by changing its mass, shape, or internal structure, the latter associated with fibre reorientation and often denoted as *remodelling*. Moreover, in particular with regard to arterial tissue, it is well known that an externally unloaded state of the material is generallyxs associated with *residual stresses*. In this contribution, an anisotropic micromechanically motivated model that incorporates time-dependent remodelling effects and, moreover, accounts for residual stress distributions will be discussed.

2. Essential kinematics

Let the local deformation be characterised by the deformation gradient tensor $\boldsymbol{F} = \nabla_{\boldsymbol{X}} \boldsymbol{\varphi}$ with the Jacobian $J = \det(\boldsymbol{F}) > 0$ and the corresponding right Cauchy-Green deformation tensor $\boldsymbol{C} = \boldsymbol{F}^{\mathrm{t}} \cdot \boldsymbol{F}$, while their isochoric counterparts are represented as $\bar{\boldsymbol{F}} = J^{-1/3}\, \boldsymbol{F}$ and $\bar{\boldsymbol{C}} = \bar{\boldsymbol{F}}^{\mathrm{t}} \cdot \bar{\boldsymbol{F}}$. In view of the computational micro-sphere-scheme, additional kinematic relations referring to the underlying unit-sphere $\mathbb{U}^2$ are introduced. In this regard, according to [6], we make use of a non-affine stretch measure

$$\lambda = \left[\frac{1}{4\,\pi} \int_{\mathbb{U}^2} \bar{\lambda}^p \,\mathrm{d}A \right]^{1/p} , \qquad (1)$$

which can be interpreted as an averaged stretch over the unit-sphere, with p defining a non-affine stretch parameter, wherein $\bar{\lambda}$ denotes the isochoric stretch normal to $\mathbb{U}^2$.

3. Hyper-elastic micro-sphere model

Apart from the remodelling framework discussed in the next section, we adopt the well-established volumetric-isochoric split of the strain energy and decompose the isochoric part into an isotropic and an anisotropic contribution, i.e.

$$\Psi(\boldsymbol{C}, \boldsymbol{r}_i) = \Psi^{\mathrm{vol}}(J) + \Psi^{\mathrm{iso}}(\bar{\boldsymbol{C}}) + \Psi^{\mathrm{ani}}(\lambda(\bar{\boldsymbol{C}}, \boldsymbol{r}_i)) , \qquad (2)$$

wherein the volumetric and isotropic isochoric part is assumed to be represented by a nearly-incompressible neo-Hooke model.

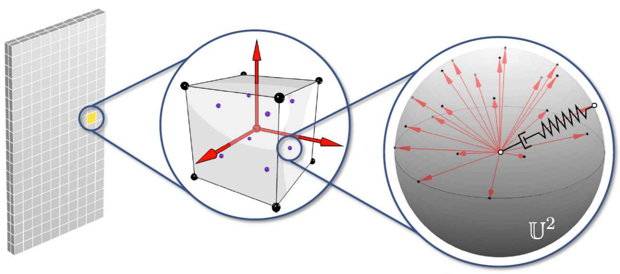

Figure 1: Illustration of the micro-sphere approach: macroscopic boundary value problem (left); particular finite element with integration points (middle); micro-sphere associated with finite number of integrations directions and one-dimensional constitutive law represented by the spring-dashpot device.

The anisotropic part is determined by means of the micro-sphere formulation, so that the macroscopic stresses can be evaluated by numerical integration referred to a finite number of unit-vectors $\boldsymbol{r}_i$, resulting in

$$\Psi^{\rm ani}(\lambda(\bar{\boldsymbol{C}}, \boldsymbol{r}_i)) = \frac{1}{4\,\pi}\int_{\mathbb{U}^2} \psi^{\rm ani}(\lambda(\bar{\boldsymbol{C}}, \boldsymbol{r}_i))\,{\rm d}A\,, \tag{3}$$

where the anisotropic fibre-related part $\psi^{\rm ani}$ is characterised by means of a worm-like chain model as discussed further in [1]. An illustration of the micro-sphere approach is given in figure 1.

4. A remodelling formulation

One key aspect of this contribution consists in incorporating remodelling-phenomena by setting up deformation-driven evolution equations for the integration directions $\boldsymbol{r}_i$, so that these do not remain constant but evolve in time. To be specific, we directly relate the integration directions—now taking the interpretation as internal variables—to the computational remodelling framework, i.e. the integration of equation (3) which algorithmically leads to a summation over m integration directions

$$\Psi^{\rm ani}(\lambda(\bar{\boldsymbol{C}}, \boldsymbol{r}_i)) \approx \sum_{i=1}^{m} w_i\,\psi^{\rm ani}(\lambda(\bar{\boldsymbol{C}}, \boldsymbol{r}_i)), \tag{4}$$

with w_i denoting integration factors which depend on the particular integration scheme.

Since various biological tissues show fibre alignment with more than one single direction, we subsequently propose a remodelling formulation reflecting macroscopically orthotropic behaviour. A detailed discussion can be found in [4], whereas an analogous approach for the transversely isotropic case has recently been elaborated in [5].

In view of the reorientation formulation, a key point consists in the identification of the deformation-dependent mean directions $\boldsymbol{l}_{1,2}$, which should determine the alignment of the integration directions $\boldsymbol{r}_i$ on the one hand and is here assumed to reflect extremal states of strain energy on the other. In this context, we make use of two particular directions reported in [2]: the so-called limiting directions, which—for the subsequently investigated example— can be calculated via

$$\boldsymbol{l}_{1,2} = \frac{\sqrt{\lambda_1^{\bar{C}}}\,\boldsymbol{n}_2^{\bar{C}} \pm \sqrt{\lambda_2^{\bar{C}}}\,\boldsymbol{n}_1^{\bar{C}}}{\sqrt{\lambda_1^{\bar{C}} + \lambda_2^{\bar{C}}}} \quad \text{for} \quad \lambda_1^{\bar{C}} > \lambda_2^{\bar{C}} > 1 \tag{5}$$

with $\bar{\boldsymbol{C}} = \sum_{j=1}^{3} \lambda_j^{\bar{C}}\boldsymbol{n}_j^{\bar{C}} \otimes \boldsymbol{n}_j^{\bar{C}}$ and $\lambda_1^{\bar{C}} > \lambda_2^{\bar{C}} > \lambda_3^{\bar{C}}$ using the principal values $\lambda_{1,2}^{\bar{C}}$ and principal directions $\boldsymbol{n}_{1,2}^{\bar{C}}$ of the isochoric right Cauchy-Green deformation tensor $\bar{\boldsymbol{C}}$. Practically speaking, these limiting directions suffer the maximum shear in the considered plane of tension. The evolution of $\boldsymbol{r}_i$ is motivated by its alignment with the limiting directions $\boldsymbol{l}_{1,2}$ as reflected by

$$\dot{\boldsymbol{r}}_i = f\ \text{sign}\,(\boldsymbol{r}_i\cdot\boldsymbol{l})\ [\boldsymbol{l} - [\boldsymbol{r}_i\cdot\boldsymbol{l}]\,\boldsymbol{r}_i] \quad \text{so that} \quad \dot{\boldsymbol{r}}_i\cdot\boldsymbol{r}_i = 0\,, \tag{6}$$

where the integration direction $\boldsymbol{r}_i$ aligns either with $\boldsymbol{l}_1$ in case of $\boldsymbol{r}_i$ being closer to $\boldsymbol{l}_1$ or else with $\boldsymbol{l}_2$. , i.e.

$$\boldsymbol{l} = \begin{cases} \boldsymbol{l}_2 & \text{if} \quad |\boldsymbol{r}_i\cdot\boldsymbol{l}_1| \le |\boldsymbol{r}_i\cdot\boldsymbol{l}_2| \\ \boldsymbol{l}_1 & \text{otherwise} \end{cases} \,. \tag{7}$$

Due to the alignment with respect to two mean directions, two second-order generalised structural tensors are introduced as $\boldsymbol{A}^{1,2} = \sum_{i=1}^{m} w_i\,\boldsymbol{r}_i \otimes \boldsymbol{r}_i\ \forall\ \boldsymbol{r}_i \to \boldsymbol{l}_{1,2}$. In order to visualise local anisotropic material properties later on, the orientation-distribution-type function (odf) $\rho^A = \rho^{A^1} \cup \rho^{A^2}$ is introduced with $\rho^{A^{1,2}} = \boldsymbol{e}\cdot\boldsymbol{A}^{1,2}\cdot\boldsymbol{e}$ for $\boldsymbol{e} \in \mathbb{U}^2$.

5. Incorporation of residual stresses

The second key aspect of this contribution is associated with the incorporation of residual stresses. Experimentally, residual (circumferential) stresses can be revealed by the *opening angle experiment*, where a short ring of an artery is cut in axial direction. The remaining (residual) stresses through the artery cause the ring to spring open to form an open sector.

The procedure employed here is based on a multiplicative decomposition of the total deformation gradient. To be specific, we consider a stress-free reference configuration $\mathcal{B}_0$, a load-free (but residually stressed) configuration $\mathcal{B}_{\rm res}$ and a current configuration $\mathcal{B}_t$. In this regard, we introduce a deformation gradient-type tensor $\boldsymbol{F}_0$ as a tangent mapping of the stress-free reference configuration $\mathcal{B}_0$ to the residually stressed configuration $\mathcal{B}_{\rm res}$ on the one hand and another deformation gradient-type tensor $\nabla_{\boldsymbol{X}}\boldsymbol{\varphi}$ as a mapping of the residually stressed configuration $\mathcal{B}_{\rm res}$ to the current configuration $\mathcal{B}_t$ on the other. The resulting deformation gradient tensor can then be written as

$$\boldsymbol{F} := \nabla_{\boldsymbol{X}}\boldsymbol{\varphi}\cdot\boldsymbol{F}_0\,. \tag{8}$$

Similar to the approach proposed in [3], the opening angle experiment can be reproduced by choosing the deformation gradient $\boldsymbol{F}_0$ as a function of the principal stretches and orthonormal base vectors, say $\boldsymbol{E}_{\Theta,Z,R}$ and $\boldsymbol{e}_{\theta,z,r}$, referred to the opened and closed configurations corresponding to the analytical solution of a cylindrical tube subjected to pure bending. To be specific,

$$\boldsymbol{F}_0 = \lambda_\theta\boldsymbol{e}_\theta\otimes\boldsymbol{E}_\Theta + \lambda_z\boldsymbol{e}_z\otimes\boldsymbol{E}_Z + \lambda_r\boldsymbol{e}_r\otimes\boldsymbol{E}_R\,, \tag{9}$$

where the radial stretch can be expressed as $\lambda_r = [\lambda_\theta\lambda_z]^{-1}$ reflecting the incompressibility constraint. With these relations at hand, the underlying principal stretches turn out as functions of the radii in the open and closed configurations, R and r, respectively, and the parameter $\kappa = 2\pi/[2\pi-\alpha]$, which itself is directly related to the opening angle α, i.e.

$$\lambda_r(R) = \frac{\partial r}{\partial R} = \frac{R}{r\kappa\lambda_z}\,, \qquad \lambda_\theta(R) = \frac{r}{R}\frac{\partial\theta}{\partial\Theta} = \frac{r\kappa}{R} \tag{10}$$

The technique described above also allows to include different opening angles for the distinct arterial layers within only one simulation. Apparently, for tube-like geometries this approach turns out to be rather efficient compared to imposing residual stresses by means of a numerical inverse reproduction of the opening angle method.

References

[1] V. Alastrué, M.A. Martínez, M. Doblaré and A. Menzel. Anisotropic micro-sphere-based finite elasticity applied to blood vessel modelling. *J. Mech. Phys. Solids*, 57:178-203 (doi:10.1016/j.jmps.2008.09.005), 2009.

[2] Ph. Boulanger, M. Hayes. On finite shear. *Arch. Ration. Mech. Anal.*, 151:125-185, 2000.

[3] G.A. Holzapfel, T.C. Gasser and R.W. Ogden. A new constitutive framework for arterial wall mechanics and a comparative study of material models. *Journal of Elasticity*, 61:1-48, 2000.

[4] A. Menzel, T. Waffenschmidt and V. Alastrué. An anisotropic micro-sphere approach applied to the modelling of soft biological tissues. *In: G. Kreiss et al. (eds.), Numerical Mathematics and Advanced Applications, Part 2*, 637-644, (doi: 10.1007/978-3-642-11795-4_68), 2009.

[5] A. Menzel, T. Waffenschmidt. A micro-sphere-based remodelling formulation for anisotropic biological tissues. *Phil. Trans. R. Soc. A*, 367(1902):3499-3523 (doi: 10.1098/rsta.2009.0103), 2009.

[6] C. Miehe, S. Göktepe and F. Lulei. A micro-macro approach to rubber-like materials - Part I: the non-affine micro-sphere model of rubber elasticity. *J. Mech. Phys. Solids*, 52:2617-2660, 2004.